

# Magnetic field induced global paramagnetic response in Fulde-Ferrell superconducting strip

P. M. Marychev,<sup>1</sup> V. D. Plastovets,<sup>1,2,3</sup> and D. Yu. Vodolazov<sup>1</sup>

<sup>1</sup>*Institute for Physics of Microstructures, Russian Academy of Sciences, 603950, Nizhny Novgorod, GSP-105, Russia*

<sup>2</sup>*Lobachevsky State University of Nizhny Novgorod, Nizhny Novgorod, 603950 Russia*

<sup>3</sup>*Sirius University of Science and Technology, 1 Olympic Ave, 354340 Sochi, Russia*

We theoretically study magnetic response of a superconductor/ferromagnet/normal-metal (SFN) strip in an in-plane Fulde-Ferrell (FF) state. We show that unlike to ordinary superconducting strip the FF strip can be switched from diamagnetic to paramagnetic and then back to diamagnetic state by *increasing* the perpendicular magnetic field. Being in paramagnetic state FF strip exhibits magnetic field driven second order phase transition from FF state to the ordinary state without spatial modulation along the strip. We argue that the global paramagnetic response is connected with peculiar dependence of sheet superconducting current density on supervelocity in FF state and it exists in nonlinear regime.

PACS numbers:

## INTRODUCTION

The diamagnetic Meissner effect, together with zero resistivity, is the fundamental property of superconducting state. When one places a superconducting specimen in a weak magnetic field, screening supercurrents expel magnetic flux from the interior of superconductor that leads to its diamagnetic response. However, there are experimental observations of so called paramagnetic Meissner effect (PME) in high- $T_c$  superconductors [1, 2] and disks of conventional superconductors [3, 4]. But in all these cases anomalous paramagnetic response was observed only upon cooling in low magnetic fields and was absent upon cooling without applied field. For granular high- $T_c$  superconductors the PME can be explained by the presence of the  $\pi$ -junctions [5], while in the other cases the PME is caused by the trapped flux on intrinsic inhomogeneities or surface [6, 7].

Paramagnetic response without the captured flux (vortices) can be realized in case of unusual Cooper pairing, namely the odd-frequency superconductivity. Odd-frequency pairs formally have negative density that leads to paramagnetic supercurrents and, consequently, local paramagnetism [8]. Odd-frequency superconducting state can be realized in ferromagnet part of hybrid superconductor/ferromagnet (SF) structures [9], near the normal metal/p-wave superconductor (NS) interfaces [10] and near the surface of d-wave superconductors [11]. Local paramagnetic response of odd-frequency superconductivity was directly observed in SFN trilayer [12] via measurement of enhanced magnetic field in normal layer. Also paramagnetic response of normal metal was seen at ultra-low temperatures in hybrid superconductor/normal metal structure [13] which could be explained by presence of dilute magnetic impurities leading to odd-frequency superconductivity [14].

In relatively thin SF or SFN strips the paramagnetic response of odd-frequency superconducting correlations

in F or FN layers may exceed the diamagnetic response of S layer (at proper choice of material parameters) and the in-plane Fulde-Ferrell-Larkin-Ovchinnikov (FFLO) state could be developed [15, 16]. It is modulated along the strip superconducting state and originally its existence was predicted for a bulk superconductors with spatially uniform exchange field and energy splitting of electrons with opposite spin of order of superconducting gap [17, 18]. In the FF state the superconducting order parameter has the form of the plane wave ( $\propto \exp(i\mathbf{q}_{FF}\mathbf{r})$ ) while in the LO state it is the standing wave ( $\propto \cos(\mathbf{q}_{LO}\mathbf{r})$  near  $T^{FFLO}$ ). In the pioneer works [17, 18] it was shown that the system being in the FF or LO states retains the conventional diamagnetic Meissner response at small magnetic fields.

Here we theoretically show, that magnetic response of SFN strip being in in-plane Fulde-Ferrell state is also diamagnetic at small and large fields, but there is finite range of fields where magnetic response is globally paramagnetic. It differs from global paramagnetic response predicted for small size unconventional superconducting disks [19] and thin disks/squares made of SFN trilayer [20], where it appears due to finite size effect and exists only at small fields. We argue that in case of SFN strip global paramagnetic response is connected with peculiar dependence of sheet superconducting current density on supervelocity in FF state and it appears in nonlinear regime (when dependence of superconducting current on vector potential is nonlinear). The paramagnetic response is accompanied by magnetic field driven second order phase transition from FF like state to ordinary state without spatial modulation along the strip. We also find that in presence of parallel magnetic field magnetization curves could be different depending on direction of  $\mathbf{q}_{FF}$  along the strip, which allows one to determine its direction from magnetic measurements.

## MODEL

We study magnetic response of SFN strip with length  $L$  and width  $w$  made of superconductor with thickness  $d_S$ , ferromagnet with thickness  $d_F$  and normal metal with thickness  $d_N$  (see Fig. 1). In Ref. [16] it was shown that when the ratio of resistivities  $\rho_S/\rho_N \gg 1$ , thicknesses of S and N layers are about of coherence length in superconductor and thickness of F layer is about of coherence length in ferromagnet, the in-plane Fulde-Ferrell-Larkin-Ovchinnikov state could be realized (in realistic SF hybrid this state is hard to have due to large resistivity of F layer). In our work we consider only Fulde-Ferrell like state because for studied system LO state has larger energy [21]. In bulk superconductors with spatially uniform exchange field (magnetic superconductor) LO state has smaller energy as it was found in Ref. [18]. This difference could be connected with properties of SFN trilayer, where superconducting and ferromagnetic films are thin, spatially separated and there is gradient of superconducting characteristics across the thickness of trilayer. It brings difference even between properties of Fulde-Ferrell states in SFN trilayer and magnetic superconductor. In both systems in the ground state there is finite phase gradient  $\nabla\varphi = \mathbf{q}_{FF}$  but in SFN structure there are finite superconducting currents flowing in S and FN layers in opposite directions [16] with the total (thickness integrated) zero current while in magnetic superconductor there is no spatially separated currents and both local and total currents are equal to zero.

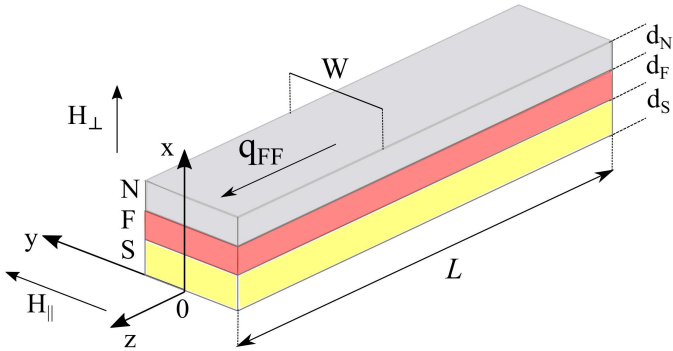


FIG. 1: The schematic representation of the SFN strip placed in parallel and perpendicular magnetic field.

To calculate the magnetization curve of SFN strip we use two models. First, we use 2D Usadel equation for normal  $g = \cos\Theta$  and anomalous  $f = \sin\Theta \exp(i\varphi)$  quasi-classical Green functions [22–24], assuming that  $\Theta$  depends only on  $x$  and  $y$  and neglect their dependence on

$z$  coordinate

$$\frac{\hbar D}{2} \left( \frac{\partial^2 \Theta}{\partial x^2} + \frac{\partial^2 \Theta}{\partial y^2} \right) - \left( (\hbar\omega_n + iE_{ex}) + \hbar \frac{D}{2} q^2 \cos \Theta \right) \sin \Theta + \Delta \cos \Theta = 0, \quad (1)$$

Here  $D$  is the diffusion coefficient of corresponding layer,  $E_{ex}$  is the exchange field which is nonzero only in F layer,  $\Delta$  is the superconducting order parameter which is nonzero only in S layer,  $\hbar\omega_n = \pi k_B T(2n+1)$  are the Matsubara frequencies ( $n$  is an integer number),  $q = \nabla\varphi + 2\pi \mathbf{A}/\Phi_0$  is the gauge invariant phase gradient that is proportional to supervelocity  $v_s \sim q$  (in this model it has only  $z$  component - see Fig. 1),  $\varphi$  is the phase of the order parameter,  $\mathbf{A}$  is the vector potential,  $\Phi_0 = \pi\hbar c/|e|$  is the magnetic flux quantum.  $\Delta$  should satisfy the self-consistency equation

$$\Delta \ln \left( \frac{T}{T_{c0}} \right) = 2\pi k_B T \sum_{\omega_n > 0} \text{Re} \left( \sin \Theta_S - \frac{\Delta}{\hbar\omega_n} \right), \quad (2)$$

where  $T_{c0}$  is the critical temperature of single S layer in the absence of magnetic field. Equation (1) are supplemented by the Kupriyanov-Lukichev boundary conditions between layers [25]

$$\begin{aligned} D_S \frac{d\Theta_S}{dx} \Big|_{x=d_S-0} &= D_F \frac{d\Theta_F}{dx} \Big|_{x=d_S+0}, \\ D_F \frac{d\Theta_F}{dx} \Big|_{x=d_S+d_F-0} &= D_N \frac{d\Theta_N}{dx} \Big|_{x=d_S+d_F+0} \end{aligned} \quad (3)$$

We assume transparent interfaces between layers and thereupon  $\Theta$  is continuous function of  $x$ . For interfaces with vacuum we use the boundary condition  $d\Theta/dn = 0$ .

Because the thickness of whole structure is much smaller than the London penetration depth  $\lambda$  of the single S layer we neglect the contribution to vector potential from screening currents. In calculations we use the following vector potential:  $\mathbf{A} = (0, 0, -H_{\parallel}x + H_{\perp}y)$ , where  $H_{\parallel}$  is the parallel and  $H_{\perp}$  is perpendicular magnetic field (see Fig. 1).

We calculate the magnetization  $\mathbf{M}$  as

$$\mathbf{M} = \frac{\mathbf{m}}{dw} = \frac{1}{2cdw} \int \int [\mathbf{r} \times \mathbf{j}_s] dx dy, \quad (4)$$

where  $\mathbf{j}_s = (0, 0, j_z)$  is the superconducting current density

$$j_z(x, y) = \frac{2\pi k_B T}{e\rho} q \sum_{\omega_n > 0} \Re(\sin^2 \Theta), \quad (5)$$

and we are interested in  $x$  component of magnetization  $M_x$ .

In numerical calculations we use the dimensionless units. The magnitude of the order parameter is normalized in units of  $k_B T_{c0}$ , length is in units of  $\xi_c = \sqrt{\hbar D_S / k_B T_{c0}}$ . The magnetic field is measured in units of  $H_s = \Phi_0 / 2\pi w \xi_c$ , magnetization  $M_x$  is in units of  $M_0 = \Phi_0 / 2\pi \xi_c^2$ . We also take in calculations that  $\lambda(0)/\xi_c = 50$ , where  $\lambda(0)$  is London penetration depth in single S layer at  $T = 0$ .

To find  $j_z$  and  $M_x$ , we numerically solve equations (1,2) with corresponding boundary conditions. To reduce the number of free parameters we assume that the resistivity of S and F layers are equal, i.e.  $\rho_S/\rho_F = 1$ , which roughly corresponds to parameters of real highly resistive S and F films. We use  $\rho_S/\rho_N = 150$  in our calculations because formation of FF state in the SFN structure needs the large ratio of resistivities of N layer and S layers [16]. It corresponds, for example, to pair NbN/Au.

The model above is not able to take into account the states with dependence of  $\Theta$  on longitudinal coordinate (for example vortex state). To obtain full in-plane distribution of the superconducting order parameter and current density, one has to solve 3D Usadel equation which is complicated problem. Instead we use the Ginzburg-Landau like approach and describe SFN structure by the 2D (in y and z directions) equations with the effective superconducting order parameter  $\Psi$  averaged over the thickness of SFN trilayer [20]. The GL free energy functional describing 2D superconductor being in the FFLO phase was proposed in Ref. [26]

$$\begin{aligned} \tilde{F} = & \alpha(T)|\tilde{\Psi}|^2 + \frac{\beta}{2}|\tilde{\Psi}|^4 + \gamma(|\Pi_y \tilde{\Psi}|^2 + |\Pi_z \tilde{\Psi}|^2) \quad (6) \\ & + \delta(|\Pi_y^2 \tilde{\Psi}|^2 + |\Pi_z^2 \tilde{\Psi}|^2 + |\Pi_y \Pi_z \tilde{\Psi}|^2 + |\Pi_z \Pi_y \tilde{\Psi}|^2), \end{aligned}$$

where  $\tilde{\Psi}$  is a complex superconducting order parameter and  $\Pi_{y,z} = \nabla_{y,z} + i2\pi A_{y,z}/\Phi_0$ . One has to define the signs of phenomenological parameters:  $\alpha, \gamma < 0$  and  $\beta, \delta > 0$  to have Fulde-Ferrell state as a ground one [27, 28]. We have to stress that for SFN trilayer this functional was not derived from microscopic theory and we use it as phenomenological one.

The dimensionless free energy  $F$  and order parameter  $\Psi$  are introduced as:  $F = F_{GL} \tilde{F} = (\alpha^2/\beta) \tilde{F}$ ,  $\Psi = \Psi_0 \tilde{\Psi} = \sqrt{|\alpha|/\beta} \tilde{\Psi}$ , with the characteristic length  $\xi_{GL} = \sqrt{|\gamma|/|\alpha|}$  and the dimensionless parameter  $\zeta = |\alpha|\delta/|\beta|^2$ . Varying  $\int F dS$  with respect to  $\tilde{\Psi}^*$  we obtain the Ginzburg-Landau equation for the dimensionless order parameter:

$$\begin{aligned} & \zeta \{ \Pi_y^4 + \Pi_y^2 \Pi_z^2 + \Pi_z^2 \Pi_y^2 + \Pi_z^4 \} \Psi \\ & + \{ \Pi_y^2 + \Pi_z^2 \} \Psi + \Psi |\Psi|^2 - \Psi = 0. \end{aligned} \quad (7)$$

Equation (7) is supplemented by the boundary conditions

$$\Pi \Psi \Big|_n = 0, \quad \Pi^3 \Psi \Big|_n = 0. \quad (8)$$

which provide vanishing of normal component of superconducting current  $j_s|_n$  and supermomentum  $q|_n =$

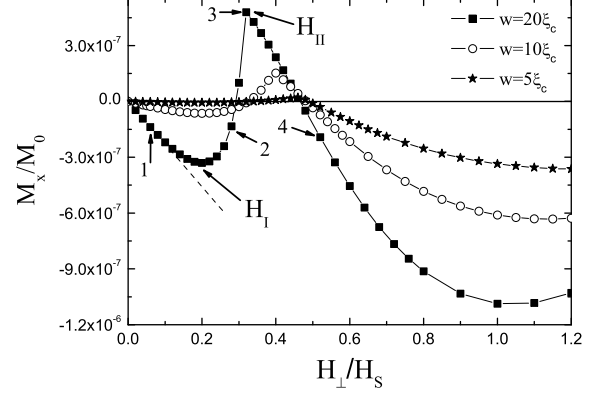


FIG. 2: The magnetization curves of SFN strips with different widths, found from Usadel model. At  $H_\perp = H_I$  there is a local minimum in dependence  $M_x(H_\perp)$ . At field  $H_\perp = H_{II}$  there is second order transition from the state with  $\overline{q_z} \neq 0$  ( $H_\perp < H_{II}$  - FF like state) to the state with  $\overline{q_z} = 0$  ( $H_\perp \geq H_{II}$  - ordinary state). Numbers 1-4 indicate fields, at which distribution of sheet current density over the width of SFN strip is shown in Fig. 3(a). The parameters of SFN strips are following:  $w = 5, 10, 20\xi_c$ ,  $d_S = 1.1\xi_c$ ,  $d_F = 0.5\xi_c$ ,  $d_N = \xi_c$ ,  $E_{ex} = 5k_B T_{c0}$  and  $T = 0.2T_{c0}$ .

$(\nabla\varphi + 2\pi A/\Phi_0)|_n$  on the boundary of FF strip with vacuum [20].

In GL model we find  $M_x$  by numerical differentiation of  $F_{GL}(H_\perp)$

$$M_x = -\frac{dF_{GL}}{dH_\perp}. \quad (9)$$

In principle, the same could be done in Usadel model too, without using of Eq. (4), but it needs small step in  $H_\perp$  and very large calculation time. It is the reason why we use different methods to find  $M_x(H_\perp)$  in Usadel and GL models.

We use relaxation method with adding of the time derivative  $\partial\Psi/\partial t$  in the right hand side of Eq. (7) and looking for  $\Psi(y, z)$  which does not depend on time. In numerical calculations we put  $\zeta = 1/8, 1/2, 2, 4$ . Case  $\zeta \lesssim 1/2$  corresponds to situation when coherence length  $\xi = \xi_{GL}(2\zeta/((1+4\zeta)^{1/2} - 1))^{1/2}$  (characteristic length variation of  $|\Psi|$  in used model) is larger than  $q_{FF}^{-1} = \xi_{GL}\sqrt{2\zeta}$  while for  $\zeta \gtrsim 1/2$  we have opposite case, which corresponds to properties of SFN strip with realistic parameters.

### MAGNETIC RESPONSE OF A SFN STRIP BEING IN THE FF STATE

In Fig. 2 we present dependence  $M_x(H_\perp)$ , found in Usadel model, for the SFN strips with different widths being in FF state at  $H_\perp = 0$ . The magnetic response is

diamagnetic at small fields as in ordinary superconductors and magnetic superconductors with spatially uniform exchange field [17, 18] but at some field (we mark it as  $H_I$  in Fig. 2)  $M_x$  reaches minimal value and then it becomes nonmonotonic function of  $H_\perp$  and changes sign twice. As a result there is finite range of magnetic fields where magnetic response is paramagnetic. Moreover, at field  $H_\perp = H_{II}$  (see Fig. 2) there is a kink, which is a signature of second order phase transition from the state with  $\bar{q}_z \neq 0$  ( $\bar{q}_z = \int q_z dy/w$  is width averaged  $q_z$ ) to the state with  $\bar{q}_z = 0$ .

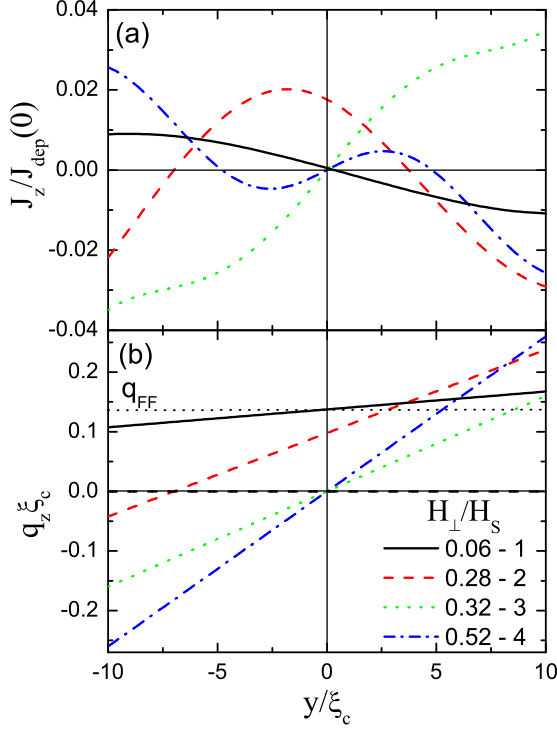


FIG. 3: (a) Distribution of sheet current density  $J_z$  and (b) supervelocity  $\sim q$  over SFN strip with width  $20\xi_c$  at different  $H_\perp$  marked by numbers 1-4 in Fig. 2. At  $H_\perp = 0.32H_s$  the  $\bar{q} = 0$ .  $J_z$  is normalized in units of  $J_{dep}(0) = j_{dep}(0)d$ , where  $j_{dep}(0)$  is depairing current density of single S layer at  $T = 0$ .

To explain this behavior in Fig. 3(a,b) we show distribution of sheet current density  $J_z = \int j_z dx$  and supervelocity  $\sim q_z$  over the width of SFN strip and in Fig. 4 dependence of  $J_z(q_z)$  in spatially homogenous case ( $q_z(y) = const$  and  $J_z(y) = const$ ). When  $H_\perp = 0$  in the ground state of FF strip there is a finite phase gradient  $\nabla\phi = q_{FF}$  but  $J_z(q_{FF}) = 0$ . From Fig. 4 one can see that near  $q_z = q_{FF}$  there is London like relation  $J_z(y) \sim J_z(q_{FF}) + (2\pi A_z(y)/\Phi_0)dJ_s/dq_z \sim -A_z(y)$  which leads to diamagnetic response of FF strip at small fields (see Fig. 2). At that fields dependence  $J_z(y)$  is

nearly odd function of  $y$  ( $J_z(y) \sim -J_z(-y)$ ) - see Fig. 3(a) for  $H_\perp = 0.06H_s$  as in ordinary strip because  $dJ_s/dq_z$  is almost constant at  $q_z \simeq q_{FF}$  - see dashed line in Fig. 4.

At larger fields due to different nonlinearity of  $J_z(q_z)$  at  $q_z < q_{FF}$  and  $q_z > q_{FF}$  the width averaged  $\bar{q}_z$  ( $\bar{q}_z(H_\perp = 0) = q_{FF}$ ) decreases, as it could be seen from Fig. 3(b), to provide zero full current  $\int J_z dy = 0$  and  $J_z(y)$  is not odd function of  $y$  (see Fig. 3(a) for  $H_\perp = 0.28H_s$ ). As a side effect it leads to nonmonotonous change of  $|M_x|$  and even to paramagnetic response because on dependence  $J_z(q)$  there is a region ( $0 < q_z < q_{c1}$ ) where  $dJ_z/dq_z > 0$ . In current driven regime with  $q_z(y) = const$  this region is not accessible [27] but it can be reached, as we find here, with coordinate dependent  $q_z(y)$ .

The  $\bar{q}_z$  goes to zero at  $H_\perp = H_{II}$  and simultaneously  $M_x$  reaches maximal positive value.  $M_x$  decreases and then changes sign at  $H_\perp > H_{II}$  while  $\bar{q}_z = 0$ . Therefore at  $H_\perp = H_{II}$  there is second order phase transition from the state with  $\bar{q}_z \neq 0$  (Fulde-Ferrell like state) to the state with  $\bar{q}_z = 0$  which is manifested as a kink on dependence  $M_x(H_\perp)$  (see Fig. 2).

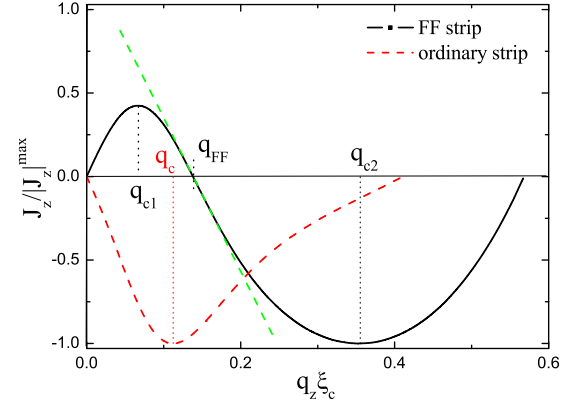


FIG. 4: Dependence of sheet current density  $J_z$  on  $q_z$  in spatially uniform case ( $J_z(y) = const$ ) for SFN strip (parameters as in Fig. 2) being in FF state and SFN strip (parameters as in Fig. 2 except  $d_F = 0.2\xi_c$ ) being in ordinary state.  $J_z$  is normalized by critical current density (it corresponds to maximal  $|J_z| = |J_z|^{max}$ ).

In ordinary superconducting strip the vortices enter the sample when supervelocity at the edge exceeds critical value ( $|\pm q_z(w/2)| \gtrsim q_c$ ) [29], except rather narrow strips with  $w \lesssim 2\xi(T)$  which do not have space for vortex [30, 31]. We expect similar behavior for FF strip too and it is the reason why we do not present  $M_x(H_\perp)$  in Fig. 2 at large fields where  $q_z(w/2)$  well exceeds  $q_{c2}$  ( $q_z(w/2) = q_{c2}$  at  $H_\perp = 0.71H_s$  for chosen parameters). But for FF strip we have additional critical value -  $q_{c1}$  (see Fig. 4). Note that  $q_z(-w/2)$  becomes smaller than  $q_{c1}$  (it occurs at  $H_\perp \lesssim H_I$ ) before  $M_x$  changes the sign,

which means that the instability may occur which breaks the homogenous along the strip state and changes dependence  $M_x(H_\perp)$ . To check it we calculate magnetic response of FF strip of finite length using Ginzburg-Landau model.

We find that while width of the strip is smaller than  $w_c \sim 2q_{FF}^{-1}$  the evolution of  $M_x$  and  $\bar{q}_z$  with magnetic field is similar to ones found from Usadel model (compare Fig. 5(a) and Fig. 2). There is a range of magnetic fields where the magnetic response is paramagnetic and at  $H = H_{II}$  there is second order transition to state with  $\bar{q}_z = 0$ . At larger fields magnetic response again becomes diamagnetic and if the width of the strip is larger than  $\sim 2\xi$  vortices enter the FF strip which leads to jumps in  $M_x$  as in ordinary superconducting strip (see Fig. 5(a)). Moreover, even relative change of magnetization is similar in Figs. 2 and 5 (if we compare, for example, maximal positive and negative  $M_x$ ). Note, that in Figs. 2 we present results found in Usadel model for SFN structure with realistic parameters, and it helps to estimate the strength of the effect (see section Summary). In Fig. 5 we present results found in GL model, where  $M_{GL}$  is some parameter which we cannot express via material characteristics of SFN structure.

For strip with  $w > w_c$  the evolution of  $M_x$  and  $\bar{q}_z$  in field range  $H_I \lesssim H_\perp \leq H_{II}$  is different. It turns out that at  $H_\perp \gtrsim H_I$  there appears finite  $q_y$  (transversal component of  $\bar{q}$ ) not only near the ends of the strip, where it provides conservation of full current, but also far from it (see insets in Fig. 5(b)). In different halves of the strip  $q_y$  has opposite sign due to different sign of the screening currents. In regions where  $q_y \neq 0$   $\bar{q}_z$  is got suppressed, depends on longitudinal ( $z$ ) coordinate and it has maximum in the center of the strip. With increasing of magnetic field  $\bar{q}_z(z)$  gradually decreases and at  $H = H_{II}$  it goes to zero along the whole strip.

Apparently, found critical width of the strip  $w_c \sim 2q_{FF}^{-1}$  is correlated with critical length of quasi 1D FF superconductor  $L_c = \pi/\sqrt{2}q_{FF}^{-1} \simeq 2.2q_{FF}^{-1}$  when spatially modulated state with  $q \neq 0$  can appear [20]. In narrower strip the transition to state with  $\bar{q}_z = 0$  occurs homogeneously along the strip because  $\bar{q}_z$  depends on  $z$  only near the ends where  $q_z = 0$  due to boundary conditions and results found in framework of Usadel model and GL models qualitatively coincide. In wider strip  $\bar{q}_z$  strongly depends on length at  $H_\perp > H_I$  because of appearance of transversal component of  $\bar{q}$ . Obviously this result cannot be found in framework of our 2D Usadel model which assumes spatial uniformity ( $q_z(z) = \text{const}$ ) along the FF strip. It leads to quantitatively different shape of  $M_x(H_\perp)$  in field range  $H_I < H_\perp < H_{II}$  for strips with  $w > w_c$  and  $w < w_c$  (compare Fig. 5(b) with Fig. 5(a) and Fig. 2). For parameters of SFN strip those magnetic response is shown in Fig. 2  $q_{FF}^{-1} \sim 7.2\xi_c$  (see Fig. 4) and, hence, only for strip with  $w = 20\xi_c$  we can expect appearance of transversal modulation.

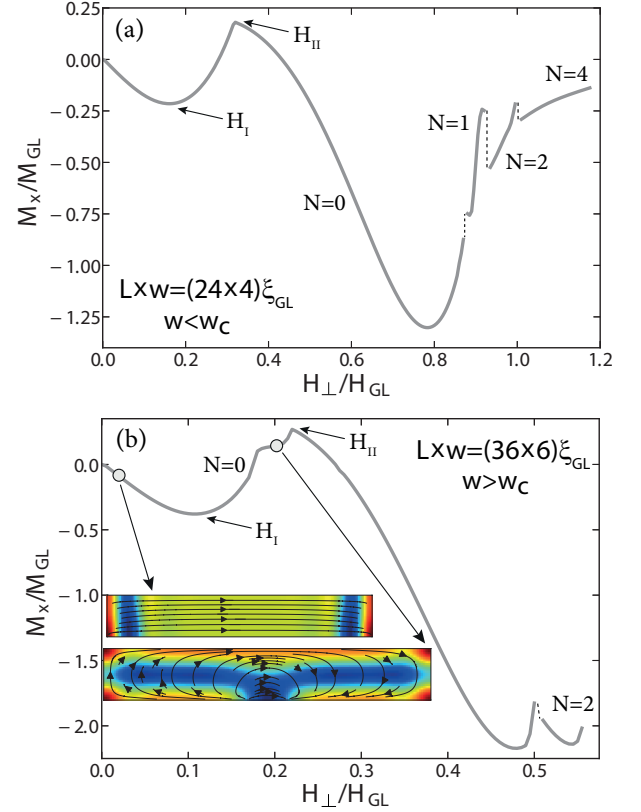


FIG. 5: Field-dependent magnetization of FF strips calculated in framework of Ginzburg-Landau model. Lateral sizes of FF strip are shown in panels (a) and (b), parameter  $\zeta = 2$  ( $q_{FF}^{-1} = 2\xi_{GL} > \xi = \sqrt{2}\xi_{GL}$ ). Magnetic field is measured in units of  $H_{GL} = \Phi_0/2\pi\xi_{GL}^2$ , magnetic moment is in units of  $M_{GL} = F_{GL}/H_{GL}$ ,  $N = \oint \nabla\varphi dl/2\pi$  is a total vorticity in the strip. In inset in (b) we show spatial distribution of  $|\Psi|$  and  $q$  at different magnetic fields.

We also find interesting behavior when  $\zeta = 1/2$  and  $1/8$  which physically correspond to  $\xi \gtrsim q_{FF}^{-1}$ . In strip with  $w \gtrsim w_c$  the transition to state with  $\bar{q}_z = 0$  starts from the ends of the strip but it is accompanied not only by appearance of finite  $q_y$  but also vortex-antivortex pairs (see insets in Fig. 6(a)). In longer strip their number increases with increasing of magnetic field and reaches the maximal value at  $H = H_{II}$  (for example when  $L = 48\xi_{GL}$  there are four vortex-antivortex pairs - not shown here). At  $H = H_{II}$  there is first order transition to state with  $\bar{q}_z = 0$  and one additional antivortex enters the strip in its center (see Fig. 6(a)). With further increase of magnetic field the number of vortex-antivortex pairs decreases one by one and at large field only vortices exist in the strip. In wider strip (see Fig. 6(b)) vortex-antivortex pairs do not appear but transition at  $H = H_{II}$  is also of first order and one antivortex enters the strip in its center which is annihilated with vortices at larger fields (see Fig. 6(b)).

In ordinary superconductors vortices and antivortices can coexist in small size (mesoscopic) samples placed

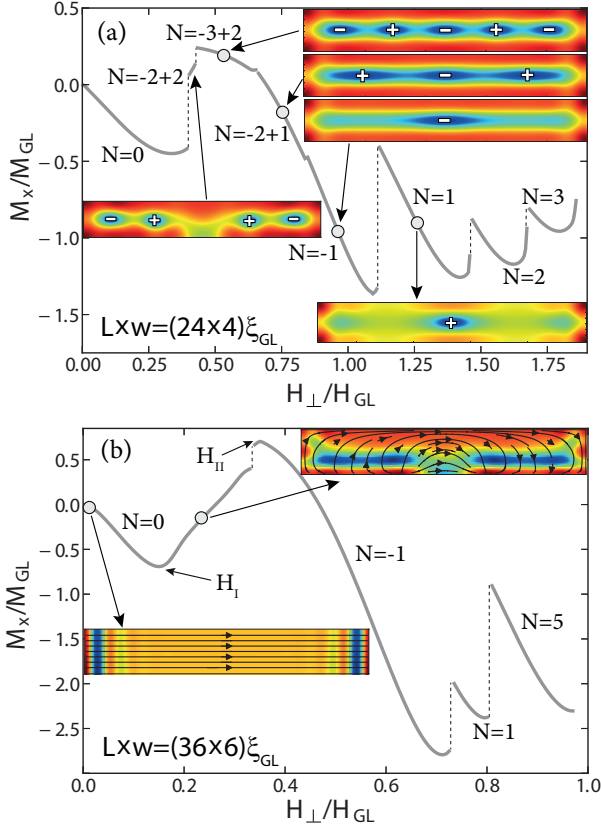


FIG. 6: Field-dependent magnetization of FF strips calculated in framework of Ginzburg-Landau model. Lateral sizes of FF strip are shown in panels (a) and (b), parameter  $\zeta = 0.5$  ( $q_{FF}^{-1} = \xi_{GL} < \xi \simeq 0.84\xi_{GL}$ ). For both panels  $w > w_c$ . In insets we show spatial distribution of  $|\Psi|$  and  $q$  at different magnetic fields. Symbols  $-$  and  $+$  indicate antivortex and vortex, correspondingly.

in external magnetic field [32–34] or near ferromagnetic domain wall where magnetic field changes the sign (experimentally such vortices and antivortices have been observed recently in ferromagnetic superconductor  $\text{EuFe}_2(\text{As}_{0.79}\text{P}_{0.21})_2$  [36]). In zero magnetic field their simultaneous appearance in the ground state was predicted in FFLO system with two coupled superconducting order parameters [35] and as a metastable state they may exist in small size FF superconductor [20]. We find that in FF strip vortex-antivortex chain is a ground state in finite range of the magnetic fields when  $w \gtrsim w_c$  and  $\xi \gtrsim q_{FF}^{-1}$ .

Using Usadel approach we also calculate dependence  $M_x(T)$  at fixed  $H_\perp$  and  $M_x(H_\perp)$  at different temperatures (see Fig. 7). We use the same parameters as in Fig. 2, except thickness of S layer was chosen  $d_S = 1.4\xi_c$ , for which the transition temperature to FF state  $T^{FF}$  is below the critical temperature of trilayer  $T_c = 0.62T_{c0} > T^{FF} = 0.38T_{c0}$ . It can be seen that  $M_x(T)$  at small fields is nonmonotonous even at  $T > T^{FF}$ , which is consequence of existence of paramagnetic currents in FN lay-

ers, while the global magnetic response is diamagnetic for all fields when  $T > T^{FF}$  (see Fig. 7(b)).

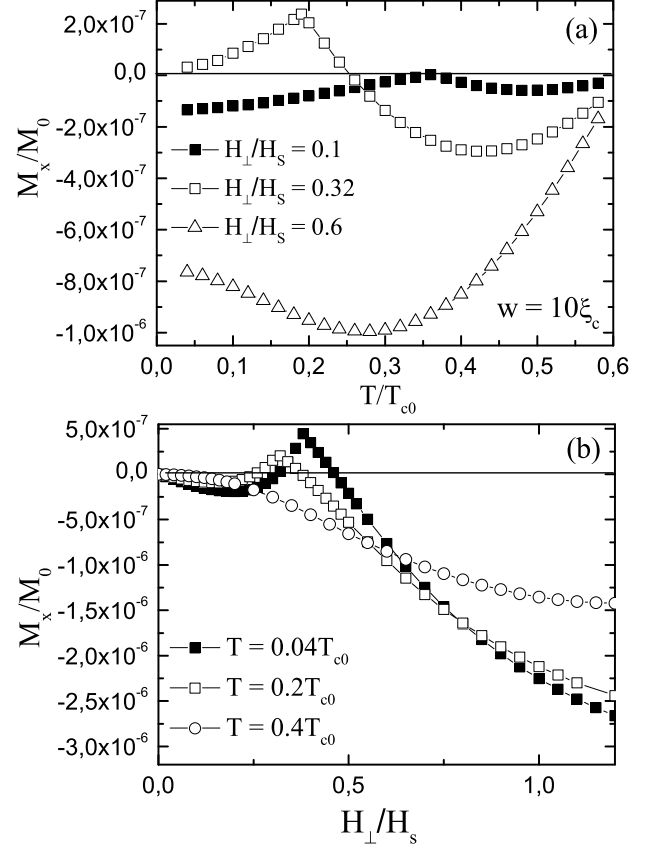


FIG. 7: (a) Dependence of the magnetization of SFN strip on the temperature at different values of the perpendicular magnetic field. (b) The magnetization curve of the SFN strip at different temperatures. We use the same parameters of SFN strip as in Fig. 2 except  $d_S = 1.4\xi_N$  and choose  $w = 10\xi_c$ . The temperature of transition to the FF state is  $T^{FF} = 0.38T_{c0}$ , critical temperature of SFN trilayer is  $T_c = 0.62T_{c0}$  (both at  $H_\perp = 0$ ).

In the absence of parallel magnetic field the ground FF state is two-fold degenerative due to existence of two states with opposite directions of  $\mathbf{q}_{FF}$  along the strip and for both directions magnetization curves  $M_x(H_\perp)$  coincide. In Ref. [21] it was shown that parallel magnetic field removes this degeneracy and makes the state with  $H_\parallel \times \mathbf{q}_{FF} \uparrow \downarrow x$  more favorable while the other state has larger energy (it becomes unstable at relatively low but finite  $H_\parallel^*$ ). It results to different  $M_x(H_\perp)$  for states with opposite  $\mathbf{q}_{FF}$  at fixed  $H_\parallel$  or vice versus. In Fig. 8 we show this effect. Metastable state becomes unstable at some  $H_\perp$  and SFN strip switches to ground state. Note that abrupt change in magnetization is not connected with vortex entrance or exit but it occurs due to change of direction of  $\bar{\mathbf{q}}$ .



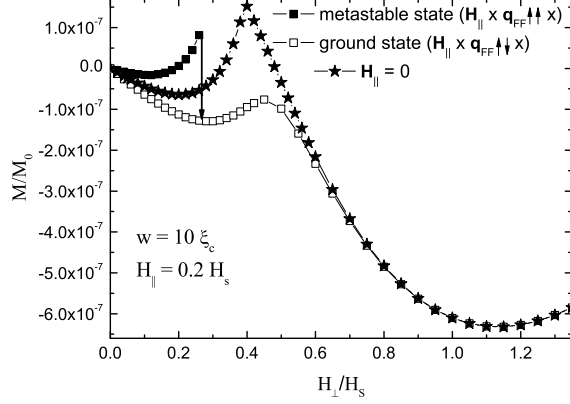


FIG. 8: The magnetization curves of SFN strip being in ground and metastable FF states (having opposite  $\mathbf{q}_{FF}$ ) which are controlled by parallel magnetic field. For comparison we also present  $M_x(H_\perp)$  when  $H_\parallel = 0$ . The arrow indicates the direction of magnetization jump which occurs with increase of  $H_\perp$ . Width of SFN strip  $w = 10\xi_c$ ,  $H_\parallel = 0.2H_s$ , the other parameters are as in Fig. 2. At  $H_\parallel > H_\parallel^* \simeq 0.4H_s$  and  $H_\perp = 0$  there is only state with  $H_\parallel \times \mathbf{q}_{FF} \uparrow\downarrow x$ .

## SUMMARY

We show that the SFN strip being in spatially modulated (Fulde-Ferrell like) ground state has global paramagnetic response in finite range of perpendicular magnetic fields, while at low and large fields the response is diamagnetic. We demonstrate that the found evolution of magnetic response with increasing of magnetic field is accompanied by vanishing of the width averaged longitudinal phase gradient  $\overline{q_z}$  which is equal to  $q_{FF}$  at zero magnetic field. We argue that both paramagnetic response and vanishing of  $\overline{q_z}$  are related and they are connected with peculiar dependence of sheet superconducting current density on supervelocity (phase gradient) in FF state.

In relatively narrow SFN strip with width  $w < w_c \sim 2q_{FF}^{-1}$ , the transition from the state with  $\overline{q_z} \neq 0$  to state with  $\overline{q_z} = 0$  at field  $H_\perp = H_{II}$  is of second order and it occurs uniformly along the strip (except its ends). At this field the paramagnetic response is maximal. In wider strip ( $w > w_c$ ) this transition is accompanied by appearance of spatial modulation of both phase and magnitude of the superconducting order parameter across the width which leads to quantitative modification of the magnetic response. Calculations in framework of Ginzburg-Landau model show that the transition of the FF strip with width  $w \gtrsim w_c$  and  $\xi \gtrsim q_{FF}^{-1}$  to state with  $\overline{q_z} = 0$  starts from appearance of vortex-antivortex pairs near the ends of the strip and ends up by formation of vortex-antivortex chain before the first order transition occurs at  $H_\perp = H_{II}$ . At fields  $H_\perp \gg H_{II}$  both narrow and wide FF strips be-

have as ordinary superconducting strip - they have diamagnetic response and number of vortices increases with increase of  $H_\perp$ .

Parallel magnetic field removes the degeneracy, connected with two directions of  $\mathbf{q}_{FF}$  along the SFN strip. It results to different magnetization curves  $M_x(H_\perp)$  depending on parallel or antiparallel orientation of vector  $H_\parallel \times \mathbf{q}_{FF}$  and normal vector to surface of SFN strip.

Using parameters of NbN as S layer ( $\rho_S = 200\mu\Omega \cdot \text{cm}$ ,  $D_S = 0.5\text{cm}^2/\text{s}$ ,  $T_{c0} = 10\text{K}$ ) and Au as N layer ( $\rho_N = 2\mu\Omega \cdot \text{cm}$ ) we can estimate geometrical parameters of SFN strip and value of paramagnetic response (any ferromagnetic material could be used as a F layer if it stays ferromagnetic when its thickness is about of  $\xi_F = (\hbar D_F/E_{ex})^{1/2}$  - for example alloy CuNi [37]). For chosen materials  $\xi_c = 6.4\text{nm}$  and  $M_0 = 8T$ . From Fig. 2 it follows that for SFN strip with  $w = 20\xi_c \sim 130\text{nm}$  the maximal positive  $4\pi M_x$  is of order of a few tenth of Gauss. Therefore, to see the predicted effect the array of SFN strips should be used and SQUID magnetometer to measure their magnetization curves. We do not believe that vortex-antivortex chain may exist in SFN strip because  $q_{FF}^{-1} \gg \xi_c \sim \xi$  for this system.

When we calculate  $M_x(H_\perp)$  we assume that magnetization of F layer is not changed. In reality it may vary and it may give additional contribution to magnetic response. One way to solve this problem is to measure  $M_x(H_\perp)$  above and below  $T_c$  and than compare them. Second solution is to choose magnetic material with in-plane magnetization having no or small number of domains. To decrease  $H_\perp$  one can take wide FF strip. For example in [37] it was found well pronounced  $0-\pi$  transition in planar NbN/CuNi/NbN Josephson junction with lateral size  $10\mu\text{m} \times 10\mu\text{m}$ . This result says that at least on this scale CuNi is homogenous enough. For FF strip based on NbN/CuNi/Au with width  $1\mu\text{m}$  and  $\xi_c = 6.3\text{nm}$  we have  $H_s \sim 50\text{Oe}$  which is small enough.

Authors acknowledge support from Foundation for the Advancement of Theoretical Physics and Mathematics "Basis" (grant 18-1-2-64-2), Russian Foundation for Basic Research (project number 19-31-51019) and Russian State Contract No. 0035-2019-0021.

- 
- [1] P. Svelindh, K. Niskanen, P. Norling, P. Nordblad, L.Lundgren, B. Lonnberg, and T. Lundstrom, Anti-Meissner effect in the BiSrCaCuO-system, *Physica C* **162–164**, 1365 (1989).
  - [2] S. Riedling, G. Bruchle, R. Lucht, K. Rhberg, H. v.Lhneysen, and H. Claus, Observation of the Wohleben effect in  $\text{YBa}_2\text{Cu}_3\text{O}_{7-\delta}$  single crystals, *Phys. Rev. B* **49**, 13283 (1994).
  - [3] D. J. Thompson, M. S. M. Minhaj, L. E. Wenger, and J. T. Chen, Observation of paramagnetic Meissner effect in niobium disks, *Phys. Rev. Lett.* **75**, 529 (1995).

- [4] A. K. Geim, S. V. Dubonos, J. G. S. Lok, M. Henini, and J. C. Maan, Paramagnetic Meissner effect in small superconductors, *Nature (London)* **396**, 144 (1998).
- [5] M. Sigrist and T. M. Rice, Unusual paramagnetic phenomena in granular high-temperature superconductors-A consequence of d-wave pairing?, *Rev. Mod. Phys.* **67**, 503 (1995).
- [6] A. E. Koshelev and A. I. Larkin, Paramagnetic moment in field-cooled superconducting plates: Paramagnetic Meissner effect, *Phys. Rev. B* **52**, 13559 (1995).
- [7] V. V. Moshchalkov, X. G. Qiu, and V. Bruyndoncx, Paramagnetic Meissner effect from the self-consistent solution of the Ginzburg-Landau equations, *Phys. Rev. B* **55**, 11793 (1997).
- [8] F. S. Bergeret, A. F. Volkov, and K. B. Efetov, Josephson current in superconductor-ferromagnet structures with a nonhomogeneous magnetization, *Phys. Rev. B* **64**, 134506 (2001).
- [9] M. Alidoust, K. Halterman, and J. Linder, Meissner effect probing of odd-frequency triplet pairing in superconducting spin valves, *Phys. Rev. B* **89**, 054508 (2014).
- [10] Y. Asano, A. A. Golubov, Y. V. Fominov, and Y. Tanaka, Unconventional Surface Impedance of a Normal-Metal Film Covering a Spin-Triplet Superconductor Due to Odd-Frequency Cooper Pairs, *Phys. Rev. Lett.* **107**, 087001 (2011).
- [11] H. Walter, W. Prusseit, R. Semerad, H. Kinder, W. Assmann, H. Huber, H. Burkhardt, D. Rainer, and J. A. Sauls, Low-Temperature Anomaly in the Penetration Depth of  $\text{YBa}_2\text{Cu}_3\text{O}_7$  Films: Evidence for Andreev Bound States at Surfaces, *Phys. Rev. Lett.* **80**, 3598 (1998).
- [12] A. Di Bernardo, Z. Salman, X. L. Wang, M. Amado, M. Egilmez, M. G. Flokstra, A. Suter, S. L. Lee, J. H. Zhao, T. Prokscha, E. Morenzoni, M. G. Blamire, J. Linder, and J. W. A. Robinson, Intrinsic Paramagnetic Meissner Effect Due to s-Wave Odd-Frequency Superconductivity, *Phys. Rev. X* **5**, 041021 (2015).
- [13] F. B. Muller-Allinger and A. C. Mota, Paramagnetic Reentrant Effect in High Purity Mesoscopic AgNb Proximity Structures, *Phys. Rev. Lett.* **84**, 3161 (2000).
- [14] C. Espedal, T. Yokoyama, and J. Linder, Anisotropic Paramagnetic Meissner Effect by Spin-Orbit Coupling, *Phys. Rev. Lett.* **116**, 127002 (2016).
- [15] S. Mironov, A. Mel'nikov, and A. Buzdin, Vanishing Meissner effect as a Hallmark of in-Plane Fulde-Ferrell-Larkin-Ovchinnikov Instability in Superconductor-Ferromagnet Layered Systems, *Phys. Rev. Lett.* **109**, 237002 (2012).
- [16] S. V. Mironov, D. Vodolazov, Yu. Yerin, A. V. Samokhvalov, A. S. Melnikov, and A. Buzdin, Temperature Controlled Fulde-Ferrell-Larkin-Ovchinnikov Instability in Superconductor-Ferromagnet Hybrids, *Phys. Rev. Lett.* **121**, 077002 (2018).
- [17] P. Fulde and R. A. Ferrell, Superconductivity in a strong spin-exchange field, *Phys. Rev.* **135**, A550 (1964).
- [18] A. I. Larkin and Yu. N. Ovchinnikov, Inhomogeneous state of superconductors, *Zh. Eksp. Teor. Fiz.* **47**, 1136 (1964) [*Sov. Phys. JETP* **20**, 762 (1965)].
- [19] S. I. Suzuki and Y. Asano, Paramagnetic instability of small topological superconductors, *Phys. Rev. B* **89**, 184508 (2014).
- [20] V. D. Plastovets and D. Yu. Vodolazov, Paramagnetic Meissner, vortex, and onion-like ground states in a finite-size Fulde-Ferrell superconductor, *Phys. Rev. B* **101**, 184513 (2020).
- [21] P. M. Marychev and D. Yu. Vodolazov, Tuning the in-plane Fulde-Ferrell-Larkin-Ovchinnikov state in a superconductor/ferromagnet/normal-metal hybrid structure by current or magnetic field, *Phys. Rev. B* **98**, 214510 (2018).
- [22] A. A. Golubov, M. Yu. Kupriyanov, and E. Il'ichev, The current-phase relation in Josephson junctions, *Rev. Mod. Phys.* **76**, 411 (2004).
- [23] A. I. Buzdin, Proximity effects in superconductor-ferromagnet heterostructures, *Rev. Mod. Phys.* **77**, 935 (2005).
- [24] F. S. Bergeret, A. F. Volkov, and K. B. Efetov, Odd triplet superconductivity and related phenomena in superconductor-ferromagnet structures, *Rev. Mod. Phys.* **77**, 1321 (2005).
- [25] M. Yu. Kupriyanov and V. F. Lukichev, Influence of boundary transparency on the critical current of "dirty" SS'S structures, *Sov. Phys. JETP* **67**, 1163 (1988).
- [26] A. Buzdin, Y. Matsuda and T. Shibauchi, FFLO state in thin superconducting films, *Europhys. Lett.* **80**, 67004 (2007).
- [27] K. V. Samokhin, B. P. Truong, Current-carrying states in Fulde-Ferrell-Larkin-Ovchinnikov superconductors, *Phys. Rev. B* **96**, 214501 (2017).
- [28] V. D. Plastovets and D. Y. Vodolazov, Dynamics of Domain Walls in a Fulde-Ferrell Superconductor, *JETP Lett.* **109**, 729 (2019).
- [29] D. Yu. Vodolazov, I. L. Maksimov, E. H. Brandt, Vortex entry conditions in type-II superconductors. Effect of surface defects, *Physica C*, **384**, 211 (2003) (2002).
- [30] H. J. Fink, Vortex Nucleation in a Superconducting Slab near a Second-Order phase Transition and Excited States of the Sheath near  $H_{c3}$ , *Physical Review* **177**, 732 (1969).
- [31] D. Saint-James, G. Sarma and E. J. Thomas, Type II superconductivity, Pergamon Press (1969).
- [32] L. F. Chibotaru, A. Ceulemans, V. Bruyndoncx, and V. V. Moshchalkov, Symmetry-induced formation of antivortices in mesoscopic superconductors, *Nature* **408**, 833 (2000).
- [33] A. S. Mel'nikov, I. M. Nefedov, D. A. Ryzhov, I. A. Shereshevskii, V. M. Vinokur, P. P. Vysheslavtsev, Vortex states and magnetization curve of square mesoscopic superconductors, *Phys. Rev. B* **65**, 140503, (2002).
- [34] V. R. Misko, V. M. Fomin, J. T. Devreese, and V. V. Moshchalkov, Stable Vortex-Antivortex Molecules in Mesoscopic Superconducting Triangles, *Phys. Rev. Lett.* **90**, 147003 (2003).
- [35] A. Samoilienka, F. N. Rybakov, and E. Babaev, Synthetic nuclear Skyrme matter in imbalanced Fermi superfluids with a multicomponent order parameter, *Phys. Rev. A* **101**, 013614 (2020).
- [36] V. S. Stolyarov, I. S. Veshchunov, S. Yu. Grebenchuk, D. S. Baranov, I. A. Golovchanskiy, A. G. Shishkin, N. Zhou, Z. Shi, X. Xu, S. Pyon, Y. Sun, W. Jiao, G.-H. Cao, L. Ya. Vinnikov, A. A. Golubov, T. Tamegai, A. I. Buzdin, D. Roditchev, Domain Meissner state and spontaneous vortex-antivortex generation in the ferromagnetic superconductor  $\text{EuFe}_2(\text{As}_{0.79}\text{P}_{0.21})_2$ , *Science Advances* **4**, 1061 (2018).
- [37] T. Yamashita, A. Kawakami, and H. Terai, NbN-Based Ferromagnetic 0 and  $\pi$  Josephson Junctions, *Phys. Rev. Applied* **8**, 054028 (2017).